Predicting the effect of pressure on biodiesel density at pressures of up to 200 MPa based on fatty acid alkyl ester profiles and density values at atmospheric pressure

Jean-Luc Daridon

Predicting the effect of pressure on biodiesel density at pressures of up to 200 MPa based on Fatty Acid Alkyl Ester profiles and density values at atmospheric pressure

Jean-Luc Daridon

Laboratoire des Fluides Complexes et leurs Reservoirs, Universite de Pau et des Pays de l'Adour, E2S UPPA, CNRS, TOTAL, LFCR, Pau, France

ABSTRACT:

The purpose of the current study is to propose a procedure to predict the effect of pressure on biodiesel density based on fatty acid alkyl ester profiles and density values at atmospheric pressure. Based on a Murnaghan equation of state to describe the effects of pressure on density and a group-contribution method to factor in the diversity of fatty acid alkyl ester components in biodiesels, the method is applicable up to 200 MPa in a wide temperature range from 280 to 400 K. Comparison of results with experimental data show that the method provides reliable high pressure predictions for biodiesels and biodiesel blends. Typical deviations calculated between the proposed method and experimental data are 0.05% for Fatty Acid Methyl Esters and 0.04% for Fatty Acid Ethyl Esters in terms of Average Absolute Deviation, with maximum deviations of the same order of magnitude as those of experimental uncertainties.

Keywords:

Biodiesel, Fatty acid methyl ester, Fatty acid ethyl ester, density, compressibility, pressure

1. Introduction

Biodiesel is a renewable, biodegradable and non-toxic diesel engine fuel, designated B100 and simply defined by standard specifications (American Society for Testing and Materials D6751 [1]). Derived from an increasing variety of raw resources such as vegetable oils, animal fats and waste cooking oils and fats, biodiesel fuels are mixtures of mono-alkyl esters of long chain fatty acids. The distribution of carbon chain lengths and the degree of unsaturation of Fatty Acid Alkyl Esters strongly depends on the feedstock sources. The esters can be produced from transesterification of fatty acids with any kind of alcohol so long as it meets the requirements of the standard specifications. Consequently, the nature of the alkyl ester (methyl ester, ethyl ester, etc.) and the fatty acid alkyl ester profile significantly differ from one biodiesel to another. This difference in biodiesel composition has a direct impact on the thermophysical properties of the fuel [2] and consequently influences engine efficiency and the content of substances potentially harmful to the environment or human health in the exhaust gases. Among fuel characteristics, volumetric property and its derivative with respect to pressure appear to play a significant part in engine performance and fuel consumption. Density acts on the conversion of volume flow-rate to mass flow-rate, and therefore affects engine power [3]. It also has an impact on the size of the atomized fuel drops during the fuel injection process. In addition, isothermal compressibility has a strong influence on fuel injection timing [4,5]. Consequently, in order to optimize injection processes or design new injection systems, it is essential to know biodiesel density and how it is affected by pressure across the entire operating pressure range of the engine. Diesel engines, fuel injection systems in particular, continue to evolve to improve overall engine performance. For better combustion efficiency, fuels are now being exposed to very high pressures in common rail direct injection systems, where the fuel is directly injected into the combustion chamber at

pressures of up to 200 MPa [6,7]. Although many studies [8-12] have been undertaken to predict the density of biodiesels as a function of temperature at atmospheric pressure or even at moderate pressures (up to 50 MPa) [13,15], few studies have been carried out at higher pressures. Consequently, the aim of the present work is to establish a correlation to predict the influence of pressure on biodiesel density up to 200 MPa across a wide temperature range from 280 to 400 K based only on Fatty Acid Methyl Ester (FAME) or Fatty Acid Ethyl Ester (FAEE) distribution profiles.

As biodiesel fuels are composed mainly of fatty acid alkyl esters ranging from methyl caprate (MC10:0) to methyl lignocerate (MC24:0) [16], i.e. components belonging to the same chemical family, excess volume is limited and biodiesel density and compressibility can be predicted from the volumetric properties of its components, assuming an ideal solution. Consequently, predicting the effect of pressure on biodiesel density amounts to correlating the density of each FAME and FAEE as a function of pressure. With this aim in mind, a Murnaghan equation [17] was considered here to represent the effect of pressure on the volumetric properties of fatty acid alkyl esters up to 200 MPa; this equation involves only two parameters, and appears as one of the most suitable for deriving compressibility from high-pressure density data [18]. For the predominant saturated and unsaturated components of biodiesels (i.e. laurate, myristate, palmitate, oleate and linoleate) these parameters can be determined by fitting density data, abundant at pressures of up to 50 MPa, 100 MPa and even up to 200 MPa. However, besides these predominant fatty acid alkyl esters, many biodiesels contain non-negligible quantities of other saturated and unsaturated components that might have an influence on density depending on the biomass feedstock used. The densities at atmospheric pressure of some of these minority components have been measured and compiled by Pratas et al. [19], but the effect of pressure on volumetric properties has received

75 little attention and no high pressure data are available. To make up for this absence of data,
76 the choice was made to set up a database from a group contribution method that would serve
77 to determine Murnaghan equation parameters for all the fatty acid alkyl ester components
78 commonly encountered in biodiesels, and therefore calculate the density of biodiesel as a
79 function of pressure based on its fatty acid alkyl ester profile. The predictive capacity of the
80 proposed method concerning the effect of pressure on biodiesel densities was tested against
81 the experimental high pressure density data available in the literature for biodiesels coming
82 from various feedstocks.
83
84
85 **2. Estimation of pure fatty acid alkyl esters densities**
86 *2.1 High pressure density data for pure fatty acid alkyl esters*
87 Predicting the influence of pressure on biodiesel density based on fatty acid alkyl ester
88 profiles requires knowing the liquid density of pure components over a wide pressure and
89 temperature range. With this aim in mind, high pressure density data available in litterature as
90 well as their temperature and pressure ranges we listed in Table 1. It can be noted in this table
91 that the data span the temperature range from 270 to 470 K and the pressure range from 0.1 to
92 200 MPa but most of the data were obtained from an oscillating U-tube density meter at
93 pressures up to 70 MPa or up to 140 MPa. Some data were determined at higher pressures by
94 integrating speed of sound measurements. Finally, two datasets were obtained using a
95 flowmeter and a piezometer respectively. As can be observed in this table, there are very few
96 high pressure density data available despite the important role they play in designing high
97 pressure fuel injection systems. A total of 4350 experimental density values were found for
98 just 11 components, 7 of which belong to the FAME family and 4 to the FAEE family. As can
99 be seen, the data available mainly concern the saturated fatty acid alkyl esters ranging from

C10:0 to C18:0 and two unsaturated fatty alkyl esters, C18:1 and C18:2. Even then, the values are not equally distributed across the *p,T* domain. Most data concern the pressure range below 100 MPa. Only few data are available up to 200 MPa. In addition to these components, most biodiesels contain non-negligible quantities of other saturated and unsaturated fatty acid alkyl esters. The densities at atmospheric pressure of some of these components were measured. Table 2 lists the components present in most biodiesels and the researchers who measured the densities of these components under atmospheric conditions. This table shows that the effect of temperature on the volumetric properties of long-chain saturated and polyunsaturated methyl esters have been extensively measured by Pratas et al. [19]. Consequently, density data obtained at atmospheric pressure across a wide temperature range are available for all components belonging to the fatty acid methyl ester family. Long-chain ethyl esters have received less attention and there is a total absence of data for some of them, such as ethyl gadoleate, behenate, erucate and lignocerate.

2.2 Representing the effect of pressure on volumetric properties

Many studies have been carried out with the aim of creating a model able to predict the volumetric behavior of liquid based on theoretical considerations, but none of them have produced a universal equation of state. Consequently, an empirical equation of state must be considered for describing the effect of pressure on liquid density. For that purpose, the following form of the Murnaghan equation [17] was used in this work:

$$\frac{\rho}{\rho_{atm}} = (1 + B\tilde{p})^{-C} \quad (1)$$

where B and C are empirical fitting parameters dependent of temperature and where $\tilde{p}$ corresponds to the relative pressure: $p - p_{atm}$. The temperature dependences of B and C are described by the polynomial forms:

$$B = b_0 + b_1 T + b_2 T^2 \quad (2)$$

$$C = c_0 + c_1 T \quad (3)$$

This equation was chosen as it adequately represents density within the limits of the pressure range investigated here. Moreover, it leads to a simple linear form of the tangent bulk modulus:

$$K = \rho\left(\frac{\partial p}{\partial \rho}\right)_T = -\frac{1}{BC}(1 + B\tilde{p}) \quad (4)$$

and consequently gives a reliable prediction of compressibility from density data:

$$\kappa_T = -\frac{BC}{1+B\tilde{p}} \quad (5)$$

The fitting parameters b_i and c_i must be obtained for each pure component by fitting the Murnaghan equation to experimental data within the expected pressure and temperature ranges of application of the proposed method: 0-200 MPa; 280-400 K. However, as mentioned in the previous paragraph, the data are not equally distributed. The data of some components such as myristate and palmitate (either methyl or ethyl) do not span the full *p,T* range investigated due to the appearance of liquid-solid phase transitions at high pressures and low temperatures. For other components, such as long-chain methyl esters, only data at atmospheric pressure are available. Finally, for some components such as long-chain ethyl esters there are simply no data at all. Consequently, the database needs to be completed by predicting values for the missing data points. Fortunately, the simple molecular structures of fatty acid methyl and ethyl esters have a limited number of functional groups, and the carbon chain lengths of ester species included in the composition of biodiesel vary very little whatever the feedstock source (C:10 to C:24). The group-contribution concept can therefore be straightforwardly applied to estimate the missing density data. Indeed, results from previous studies [40] concerning the densities of pure fatty acid alkyl esters under ambient conditions show that group-contribution methods applied to volume, such as the GCVOL

model [68, 69], are able to estimate atmospheric pressure densities with deviations of the order of 1.5% for FAEEs and of less than 1% in the case of FAME components.

The method consists in calculating the molar volume of a pure component under atmospheric pressure by a simple summation of group volume increments:

$$v^*_{atm}(T) = \sum_j N_j v_j(T) \quad (6)$$

where N_j is the number of j groups occurring in the pure component and v_j its volume contribution. The method can be extended to predict the influence of pressure on density by considering the same summation of volumes and using the Murnaghan equation to take into account the effect of pressure on volume contributions:

$$v^*(P,T) = \sum_j N_j A_j \left(1 + B_j \tilde{p}\right)^{C_j} \quad (7)$$

where B_j and C_j are function of temperature according to eqs. 2,3 and A_j is a function of temperature of the following form:

$$A_j = a_{0,j} + a_{1,j}T + a_{2,j}T^2 \quad (8)$$

This equation involves 8 parameters for each functional group, i.e. $a_{0,j}$, $a_{1,j}$, $a_{2,j}$, $b_{0,j}$, $b_{1,j}$, $b_{2,j}$, $c_{0,j}$, $c_{1,j}$ that were determined from fitting density data of pure components reported in Tables 1 and 2.

A decomposition involving five functional groups was chosen here to represent FAME and FAEE. Two were used to characterize the long alkyl chain (CH_3 and CH_2). The third group (CH=CH) focused on the degree of unsaturation. And the last two groups were added to take into account the ester contributions in FAME (CH_3COO) and FAEE (C_2H_5COO) respectively. As can be seen in Table 1, the available data is distributed across the relevant *p,T* range for each functional group. The a_i coefficients of each group were first determined from experimental data taken from Table 2, except those of alkyl groups (CH_3 and CH_2) which were taken from the GCVOL model [68] revised by Ihmels and Gmehling [69] as the present fit

give nearly the same a_i values for these groups. Parameters b_i and c_i were then determined by regression analysis of high pressure data reported in Table 1. The results of the regression are listed in Table 3.

The proposed group-contribution method helped fill in missing data and construct a comprehensive database with N_{exp} experimental data ranging from 0.1 to 200 MPa and from 280 to 400 K. From this comprehensive database, coefficients a_i, b_i and c_i were estimated for each FAME and FAEE considered in Table 1. Parameters b_i and c_i were regressed from high pressure data by minimizing the following objective function:

$$f_{HP}(b_i, c_i) = \sum_k^{N_{exp}} \left[(1 + B\tilde{p})^C - \left(\frac{\rho_{atm}}{\rho}\right)_{k,exp} \right]^2 \quad (9)$$

whereas a_i coefficients were independently fitted by minimizing the following objective function:

$$f_{atm}(a_i) = \sum_k^{N_{exp,atm}} \left[A - \left(\frac{1}{\rho_{atm}}\right)_{k,exp} \right]^2 \quad (10)$$

The values resulting from the fit are given in Table 4. To study the capacity of eq. 1 to represent the effect of pressure on density with the fitted parameter values, the average deviations AD%, the absolute average deviations AAD% and the maximum deviations MD% between calculated and experimental values of the density ratio ρ/ρ_{atm} were evaluated for each experimental dataset. The deviations observed for each component are given in Table 5. These deviations were chosen as they are completely independent from data at atmospheric pressure, and therefore it corresponds to the use of the model for the purpose of extrapolating known data at atmospheric pressure to high pressure according to:

$$\rho = \rho_{atm,exp} \left(\frac{\rho}{\rho_{atm}}\right)_{calc} = \rho_{atm,exp}(1 + B\tilde{p})^{-C} \quad (11)$$

leading to a relative uncertainty in terms of density corresponding to a quadratic summation of relative uncertainties:

$$U_r^2(\rho) = U_r^2\left(\rho_{atm,exp}\right) + U_r^2((\rho/\rho_{atm})_{calc}) \quad (12)$$

3. Predicting the effect of pressure on the volumetric properties of biodiesels

Most biodiesels are simple systems with few components that belong to the same family and whose carbon chain length generally ranges from 10 to 20. Consequently, excess volumes in biodiesels are very small and are often neglected when predicting density. In fact, the main drawbacks when predicting densities from ester profiles are uncertainty in chemical analysis and impurities. Indeed, end biodiesel products are obtained by conversion processes of feedstock oils that leave several types of impurities. After transesterification of the fatty acids with alcohol, the reaction product must be washed and purified to remove the glycerol and unconverted fatty acids from the biodiesel phase. Given that the purification processes are not 100% efficient, some impurities remain in variable proportions in biodiesels depending on their quality. Consequently, the molar volume of a biodiesel can be expressed as the sum of three contributions:

$$v^{B100} = v^{id}(1 + v_r^E + v_r^{chem}) \quad (13)$$

where v^{id} is the molar volume of the ideal solution with the exact ester profile, v_r^E is the relative excess molar volume $\left(v^E/v^{id}\right)$ and v_r^{chem} is the relative molar change caused by error in chemical composition and by impurities. Because biodiesels are composed of non-associated components belonging to a chemical family characterized by weak molecular interactions, v_r^E is limited and the effect of pressure on v_r^E therefore has extremely little impact on $v^{B100}(P)$. Furthermore, impurities lead to systematic deviations and so pressure change has little impact on v_r^{chem}. Consequently, considering that the effect of pressure on v_r^E

and v_r^{chem} is of second order on $v^{B100}(P)$, the volume of a biodiesel at a given pressure can be expressed as follows:

$$v^{B100}(P,T) = \frac{v^{id}(P,T)}{v_{atm}^{id}(T)} v_{atm}^{B100}(T) \quad (14)$$

This equation was rewritten in terms of density in order to predict the high pressure density of biodiesel based on experimental densities at atmospheric pressure $\rho_{atm}^{B100}(T)$ and on ester profiles according to:

$$\rho^{B100}(P,T) = \rho_{atm}^{B100}(T) \frac{\sum_i x_i A_i}{\sum_i x_i A_i (1+B_i \tilde{p})^{C_i}} \quad (15)$$

where x_i is the molar fraction of ester i in the biodiesel system investigated, A_i, B_i and C_i are ester parameters calculated from eqs. 8, 2 and 3 respectively using the coefficients of pure components listed in Table 4.

4. Results and discussion

Various biodiesels from different feedstocks were considered to test the predictive capacities of the proposed method. They included vegetable oils such as canola (C), cottonseed, (Ct), linseed (Ls), palm (P), rapeseed (R) and soybean (S), alga such as spirulina platensis (Asp), animal fats such as lard (L) and tallow (T) and also waste cooking oils (W) for which high pressure data are available in the literature. In addition, density data of a Purified Biodiesel (PB) and biofuel blends corresponding to palm + rapeseed (PR), soybean + rapeseed (SR), soybean + palm (SP), and soybean + rapeseed + palm (SRP) mixtures were considered in the comparative tests. Both methyl and ethyl biodiesels were included in the database. However, because there are a greater number of experimental studies on methyl esters than on ethyl

esters, a more in-depth analysis was conducted on FAMEs than on FAEEs. The fatty acid alkyl ester profiles of each biodiesel after normalization to 100 are summarized in Table 6. Eq. 15 was used to predict the densities of these biodiesels under high pressure based on their fatty acid alkyl ester profiles and densities at atmospheric pressure. The statistical comparison of these predictions with the data taken from the literature is summarized in Table 7 where the average deviations, average absolute deviation and the maximum deviation are reported for each dataset. As can be observed in Table 7, 2900 data points of 30 biodiesels were used as database for model comparison. The majority of the datasets concern FAME biodiesels and only four of them pertain to FAEE biodiesels. The database span a broad temperature range from 278 to 413 K, and pressures of up to 200 MPa. However, most of the data are within the 0.1 to 60 MPa bracket. Eight datasets span pressures of more than 60 MPa, and in this ensemble only three datasets reach the pressure limit imposed by the density correlation (200 MPa). Most of the experimental density values were obtained by direct volume change or from measurements acquired using an oscillating U-tube density meter, with an additional three datasets obtained using the speed of sound integration method. The expanded relative uncertainty Ur(ρ) reported by the authors with a level of confidence = 0.95 (kp = 2) usually stood at around 0.2% in the case of direct volume change measurements and at 0.1% in the case of measurements obtained with the oscillating U-tube density meter. Only Pratas et al. [13] reported data that are subject to uncertainties of less than 0.1%, with a claimed uncertainty of 0.1 $kg.m^3$ for the entire pressure and temperature range studied in their work. Finally, the combined expanded uncertainties of density values obtained at higher pressures of investigation using the speed of sound integration method were reported to be 0.2% up to 100 MPa and 0.3% between 100 and 200 MPa.

The comparison results in Table 7 indicate that most of the deviations are within the uncertainty values of the experimental method for the FAME biodiesels, with the exception of the biodiesel produced from rapeseed oil and studied by Kiełczynski et al. [71]. In this case, the deviation between the predictions of the correlation and the experimental data reaches 8% at 200 MPa. However, for this system, the experimental change in density caused by pressure change is much lower than the values of the pure C18:1 and C18:2, the main components of rapeseed oil biodiesels. Similarly, calculations deviate systematically by 0.5% on average with the measurements of NguyenThi et al. [75] performed on biodiesel produced from waste cooking oils. This systematic bias stems from the fact that the experimental density data reported in this reference are higher than the values of the main pure components (C16:0, C18:0 and C18:1) of this biodiesel in the same conditions. The differences, which are systematic, are probably attributable to impurities that do not belong to the FAME family. The mean absolute difference between measurements reported by the other authors for FAME biodiesels and the present correlation is 0.050%, which is within the experimental uncertainty of 0.1-0.3% claimed by the authors. Interestingly enough, this value is of the same order of magnitude as those of pure FAME (AAD=0.035%). This confirms that excess volume and impurities have a second order effect on the change in density with respect to pressure and therefore they can be taken into account only through density data at atmospheric pressure. Moreover, the overall bias being 0.02%, the model gives no under or over estimate of the pressure effect on biodiesel density.

Comparisons of experimental and predicted densities are shown in Fig. 1 for soy biodiesel, for which several experimental measurements were carried out under high pressure conditions. By examining this figure corresponding to T = 313 K, a temperature investigated in the different experimental studies, it can be seen that the proposed correlation is in very good

agreement with the different measurements whatever the pressure, from 0.1 to 200 MPa. In particular, it can be noted that the deviations are either positive or negative, which means that that there is no systematic bias in the prediction method.

Good agreement has also been found with the results reported by Tat and Van Gerpen [23] and Ivaniš et al. [72] for FAEE biodiesels (overall AD = -0.014%; overall AAD = -0.036%). However, for these biodiesels the pressure range of the experimental data is much less broad than for FAME biodiesels, with a maximum experimental pressure of 35 MPa for Tat and Van Gerpen's data [23] and 60 MPa for the data reported by Ivaniš et al [72]. The values reported by Ivaniš et al. with a standard uncertainty of ±0.1%, deviate from eq. 15 by less than 0.15% with an average deviation equal to 0.008% and absolute deviation of 0.02%; the majority of their results deviates from the correlation by less than 0.1 % and only two points have deviations of approximately 0.14%. Fig. 2 featuring the data of Ivaniš et al. shows the variation of the deviations against pressure at different temperatures. Here again, no systematic bias can be observed whatever the temperature. Deviations observed between the proposed method and the reported density data are within the reported experimental uncertainties.

Besides the correlation scheme proposed to predict the effect of pressure on the densities of FAME and FAEE biodiesels based on ester profiles and density data at atmospheric pressure, the parameters of Table 4 could be used to predict biodiesel densities at either atmospheric or high pressure based only on the ester profile using the following ideal combination rule:

$$\rho^{B100}(P,T) = \frac{\sum_i x_i M_i}{\sum_i x_i A_i (1+B_i \tilde{p})^{C_i}} \tag{16}$$

with M_i the molecular weight of the fatty acid alkyl ester *i*. This simple approach could indeed be used to calculate the density of synthetic mixtures of FAME or FAEE components, as in these types of systems excess volumes are very small, but also, and above all, because compositions are well known and impurity concentrations are very low. The major drawback

in extending the application of this simple mixing rule to biodiesels is that in real systems, impurity concentrations can be significant and have a substantial influence on density values. To illustrate this point, we have plotted on the same graph (Fig. 3) the deviations of the experimental results from the predictions of either eq. 15 or eq. 16 for two different biodiesels for which data span pressures of up to 140 MPa. The first biodiesel is the soybean oil biodiesel investigated by Aitbelale et al. [73] whose chemical composition was analyzed in detail by NMR and GC/MS analysis. It comprises 95.2% of FAME components, the main impurities being soybean oil residues. The second biodiesel is a purified biodiesel studied by Schedemann et al. [32] whose impurities are not specified but whose FAME profile, reported by the authors, is normalized to 100%. Observation of Fig. 3 shows that the use of eq. 16 instead of eq. 15 leads to a shift in deviation of 0.4% for soybean oil biodiesel [73] corresponding to the error in the prediction of density at atmospheric pressure. This shift in deviation, of only 0.03% in the case of purified biodiesel [32], is mainly attributed to the significant amount of impurities present in soybean oil biodiesel. It can be observed that the proposed correlation scheme (eq. 14) makes it possible to ignore the real nature of the impurities and to predict the effect of pressure on biodiesel density despite the presence of transesterification residues in end biodiesel products.

Finally, according to eq.5 and eq.15, the isothermal compressibility of biodiesel can be obtained from the ester profile and the parameters of Table 4 by using the following combining rule:

$$\kappa_T^{B100} = -\sum_i \phi_i \frac{B_i C_i}{1+B_i\tilde{p}} \tag{17}$$

With ϕ_i the calculated volume fraction defined as:

$$\phi_i = \frac{x_i A_i (1+B_i\tilde{p})^{C_i}}{\sum_k x_k A_k (1+B_k\tilde{p})^{C_k}} \tag{18}$$

345 As an example, deviations of compressibility determined by eqs. 17 and 18 using the
346 coefficients of Table 4 from literature values are shown in Fig. 4 as a function of pressure for
347 soybean oil biodiesel at T = 313 K. In these comparisons, the literature values were all
348 obtained from fitting the so-called Tait equation [77] and from analytically deriving it. It can
349 be observed in this figure that the deviations vary from −2% to +2% between 0.1 and 100
350 MPa and reach -4% at 200 MPa which is well within the overall uncertainty for this derivative
351 property [18]. Consequently, with the proposed procedure the accurate prediction of density
352 can be extended to the determination of its derivative with respect to pressure within the usual
353 uncertainty bracket achieved for such a property.
354
355

5. Conclusion

This article presents a computational procedure to predict the effect of pressure on biodiesel density based on fatty acid alkyl ester profiles and density data at atmospheric pressure. A Murnaghan equation was first proposed to correlate the densities of pure Fatty Acid Methyl Ester and Fatty Acid Ethyl Ester as a function of pressure. Then, based on this equation of state, and using existing high-pressure density data concerning either FAME or FAEE compounds, a group-contribution method was proposed to estimate the densities of the fatty acid alkyl ester components of biodiesels for which no high-pressure experimental data were available. Finally, a calculation scheme based on ester profiles and density values at atmospheric pressure was proposed to obtain further knowledge on density at high pressure. This method yields very accurate predictions of biodiesel densities up to 200 MPa across a wide range of temperatures from 280 to 400 K. The predictive character of the method was demonstrated for both FAME and FAEE biodiesels, for which predictions were compared to literature data. The overall mean average deviation obtained between the predictions and the experimental data for a wide variety of biodiesels including vegetable oil, animal fat and waste oil was less than 0.050% and the maximum deviations were of the same order of magnitude as the experimental uncertainties. Due to its predictive and accurate features, the method presented in this article can be considered very useful for predicting the effect of pressure on biodiesel density. It can be used to fill the experimental knowledge gap that exists for high pressure data. Besides extrapolating biodiesel density data to the high pressure range, the group-contribution method is of interest for predicting the densities of highly polyunsaturated fatty acid alkyl esters present in biodiesel fuels obtained from algal oils [78] such as methyl eicosadienoate (C20:2), methyl eicosatrienoate (C20:3), methyl eicosatetraenoate (C20:4), etc. for which no experimental data have yet been reported.

382 **References**

383

384 [1] American Society for Testing and Materials (ASTM). ASTM D6751-09. Standard
385 Specification for Biodiesel Fuel Blend Stock (B100) for Middle Distillate Fuels;
386 ASTM: West Conshohocken, PA, 2009.

387 [2] Ramos MJ, Fernández CM, Casas A, Rodríguez L, Pérez A. Influence of fatty acid
388 composition of raw materials on biodiesel properties. Bioresource Technology
389 2009;100:261–268.

390 [3] Boudy F, Seers P. Impact of physical properties of biodiesel on the injection process in
391 a common-rail direct injection system. Energy Conversion and Management
392 2009;50:2905–2912.

393 [4] Boehman AL, Morris D, Szybist J. The Impact of the Bulk Modulus of Diesel Fuels on
394 Fuel Injection Timing. Energy & Fuels 2004;18:1877-1882.

395 [5] Galle J, Defruyt S, Van de Maele C, Piloto Rodriguez R, Denon Q, Verliefde A,
396 Verhelst S. Experimental investigation concerning the influence of fuel type and
397 properties on the injection and atomization of liquid biofuels in an optical combustion
398 chamber. Biomass Bioenergy 2013;57:215–228.

399 [6] Wang X, Huang Z, Zhang W, Kuti O, Nishida K. Effects of ultra-high injection pressure
400 and micro-hole nozzle on flame structure and soot formation of impinging diesel spray.
401 Applied Energy 2011;88:1620–1628.

402 [7] Celıkten I. An experimental investigation of the effect of the injection pressure on
403 engine performance and exhaust emission in indirect injection diesel engines. Applied
404 Thermal Engineering 2003;23:2051–2060.

405 [8] Alptekin E, Canakci M. Determination of the density and the viscosities of biodiesel–
406 diesel fuel blends. Renew Energy 2008;33:2623–2630.

[9] Pratas MJ, Freitas S, Oliveira MB, Monteiro, SC, Lima AS, Coutinho, JAP. Biodiesel Density: Experimental Measurements and Prediction Models. Energy & Fuels 2011;25:2333–2340.

[10] Ramírez Verduzco LF. Density and viscosity of biodiesel as a function of temperature:empirical models. Renew Sustain En Rev 2013;19:652-665.

[11] Phankosol S, Sudaprasert K, Lilitchan S, Aryusuk K, Krisnangkura K. Estimation of density of biodiesel. Energy Fuel 2014;28: 4633-4641.

[12] Jiang S, Qi J, Hu Y Ren C, Jiang Y, Zhao Z. Predicting the Density and Viscosity of Biodiesels and Biodiesel Blends by the Regular-Solution Theory. Ind. Eng. Chem. Res. 2019;58:17038−17048.

[13] Pratas MJ, Oliveira MB, Pastoriza-Gallego MJ, Queimada AJ, Pineiro MM, Coutinho JAP. High-Pressure Biodiesel Density: Experimental Measurements, Correlation, and Cubic-Plus-Association Equation of State (CPA EoS) Modeling. Energy Fuels 2011;25:3806–3814.

[14] Prieto NMCT, Ferreira AGM, Portugal ATG, Moreira RJ, Santos JB. Correlation and prediction of biodiesel density for extended ranges of temperature and pressure. Fuel 2015;141: 23-38.

[15] Chum-in T, Sudaprasert K, Phankosol S, Lilitchan S, Aryusuk K, Krisnangkura K, Gibbs energy additivity approaches to QSPR in modeling of high pressure density and kinematic viscosity of FAME and biodiesel. Fuel Processing Technology 2017;156:385-393.

[16] Scrimgeour C. Chemistry of Fatty Acids, Bailey's industrial oil and fat products, Sixth Edition, Six Volume Set. John Wiley & Sons, Inc 2005.

[17] Murnaghan, FD. The compressibility of media under extreme pressures. Proc. Natl. Acad. Sci. U. S. A. 1944;30:244−247.

[18] Daridon JL, Bazile JP. Computation of Liquid Isothermal Compressibility from Density Measurements: An Application to Toluene. J. Chem. Eng. Data 2018;63:2162–2178.

[19] Pratas MJ, Freitas S, Oliveira MB, Monteiro SC, Lima A S, Coutinho JAP. Densities and Viscosities of Minority Fatty Acid Methyl and Ethyl Esters Present in Biodiesel. J Chem Eng Data 2011;56:2175–2180.

[20] Ndiaye EHI, Nasri D, Daridon JL. Speed of sound, density, and derivative properties of fatty acid methyl and ethyl esters under high pressure: methyl caprate and ethyl caprate. J. Chem. Eng. Data 2012;57:2667-2676.

[21] Zarska M, Bartoszek K, Dzida M. High pressure physicochemical properties of biodiesel components derived from coconut oil or babassu oil. Fuel 2014;125:144-151.

[22] Su C, Zhu C, Lai T, Wang T, Liu X, He M. Temperature and pressure dependence of densities and viscosities for binary mixtures of methyl decanoate plus n-heptane. Thermochimica Acta, 2018;670:211-218.

[23] Tat ME, Van Gerpen JH. Speed of sound and isentropic bulk modulus of alkyl monoesters at elevated temperatures and pressures. J Am Oil Chem Soc 2003;80:1249–1256.

[24] Wang X, Kang K, Lang H. High-pressure liquid densities and derived thermodynamic properties for methyl laurate and ethyl laurate. J. Chem. Thermodyn. 2016;103:310–315.

[25] Aissa MA, Ivaniš GR, Radović IR, Kijevčanin MLj. Experimental Investigation and Modeling of Thermophysical Properties of Pure Methyl and Ethyl Esters at High Pressures. Energy Fuels 2017;31:7110–7122.

[26] Habrioux M, Nasri D, Daridon JL. Measurement of speed of sound, density compressibility and viscosity in liquid methyl laurate and ethyl laurate up to 200 MPa by using acoustic wave sensors. J. Chem. Thermodynamics 2018;120:1–12.

457 [27] He M, Lai T, Liu X. Measurement and correlation of viscosities and densities of methyl
458 dodecanoate and ethyl dodecanoate at elevated pressures. Thermochimica Acta
459 2018;663:85–92.
460 [28] Ndiaye EHI, Habrioux M, Coutinho JAP, Paredes MLL, Daridon JL. Speed of sound,
461 density, and derivative properties of ethyl myristate, methyl myristate, and methyl
462 palmitate under high pressure. J. Chem. Eng. Data 2013;58:1371-1377.
463 [29] Rasulov SM, Abdulagatov IM. PVT, saturated liquid density and vapor-pressure
464 measurements of main components of the biofuels at high temperatures and high
465 pressures: Methyl palmitate. Fuel 2018;218:282–294.
466 [30] Outcalt SL. Compressed-liquid density measurements of methyl oleate and methyl
467 linoleate. J Chem Eng Data 2011;56:4239–43.
468 [31] Ndiaye EHI, Habrioux M, Coutinho JAP, Paredes MLL, Daridon JL. Speed of sound,
469 density, and derivative properties of methyl oleate and methyl linoleate under high
470 pressure. J. Chem. Eng. Data 2013;58:2345-2354.
471 [32] Schedemann A, Wallek T, Zeymer M, Maly M, Gmehling J. Measurement and
472 correlation of biodiesel densities at pressures up to 130 MPa. Fuel 2013;107:483–492
473 [33] Dzida M, Jężak S, Sumara J, Żarska M, Goralski P. High pressure physicochemical
474 properties of ethyl caprylate and ethyl caprate. J. Chem. Eng. Data 2013;58:1955-1962.
475 [34] Dzida M, Jężak S, Sumara J, Żarska M, Goralski P. High pressure physicochemical
476 properties of biodiesel components used for spray characteristics in diesel injection
477 systems. Fuel 2013;111:165-171.
478 [35] Bonhorst CW, Althouse PM, Triebold HO. Esters of Naturally Occurring Fatty Acids -
479 Physical Properties of Methyl, Propyl, And Isopropyl Esters of C-6 to C-18 Saturated
480 Fatty Acids. Ind. Eng. Chem. 1948;40:2379–2384.

[36] Gros AT, Feuge RO. Surface and Interfacial Tensions, Viscosities, and Other Physical Properties of Some n-Aliphatic Acids and their Methyl and Ethyl Esters. J. Am. Oil. Chem. Soc. 1952;29:313-317.

[37] Gouw TH, Vlugter JC. Physical Properties of Fatty Acid Methyl Esters. I. Density and Molar Volume. J. Am. Oil. Chem. Soc. 1964;41:142–145.

[38] Ortega J, Matos JS, Pena JA. Excess molar enthalpies of methyl alkanoates +n-nonane at 298.15 K. Thermochimica Acta 1990;160:337-342.

[39] Liew KY, Seng CE, Oh LL. Viscosities and Densities of the Methyl-Esters of Some N-Alkanoic Acids. J. Am. Oil. Chem. Soc. 1992;69:155–158.

[40] Pratas MJ, Freitas S, Oliveira MB, Monteiro SC, Lima AS, Coutinho JAP. Densities and viscosities of fatty acid methyl and ethyl esters. J Chem Eng Data 2010;55:3983–90.

[41] Daridon JL, Coutinho JAP, Ndiaye EHI, Paredes MLL. Novel data and a group contribution method for the prediction of the speed of sound and isentropic compressibility of pure fatty acids methyl and ethyl esters. Fuel 2013;105:466–470.

[42] Wang X, Wang X J. Chen, Experimental investigations of density and dynamic viscosity of n-hexadecane with three fatty acid methyl esters. Fuel 2016;166:553–559.

[43] Sun Y, Di G, Xia J, Wang X, Yang X, He S. Densities and excess molar volumes of methanol with three fatty acid methyl esters from 283.15 to 318.15 K. Energy Procedia 2018;152:143–148.

[44] Du W, Wang X. Density and viscosity for binary mixtures of methyl decanoate with 1-propanol, 1-butanol, and 1-pentanol. Journal of Molecular Liquids 2019;294:111647.

[45] Li D, Guo M, Wang X, Lin S, Jia W, Wang G. Measurement and correlation of density and viscosity of binary mixtures of fatty acid (methyl esters + methylcyclohexane). J. Chem. Thermodynamics 2019;137:86–93.

[46] Zhao G, Yuan Z, Yin J, Ma S. Thermophysical properties of fatty acid methyl and ethyl esters J. Chem. Thermodynamics 2019;134:195–212.

[47] Shigley JW, Bonhorst CW, Liang PM, Althouse PM, Triebold HO. Physical Characterization of a) a Series of Ethyl Esters and b) a Series of Ethanoate Esters. J. Am. Oil. Chem. Soc. 1955;32:213–215.

[48] Smith G, Bagley F. Effect of Molecular Size and Structure on the Pyrolysis of Esters. II The Journal of Organic Chemistry. 1959 24, 128-129

[49] Liew KY, Seng CE. Molal volumes of some n-fatty acids and their methyl and ethyl esters. J. Am. Oil Chem. Soc., 1992;69:734-40.

[50] Francesconi R, Comelli F. Excess molar enthalpies of binary mixtures containing acetic or propionic acid+eight ethyl alkanoates at 298.15 K. Thermochimica Acta 1998;322:63-68.

[51] Ortega J, Pl´acido J, Vidal M. Thermodynamic properties of (an ethyl ester + an n-alkane) .XI. H^E and V^E values for $\{xCH_3(CH_2)_uCOOCH_2CH_3 + (1\text{-}x)CH_3(CH_2)_{2v+1}CH_3\}$ with u=6, 7, 8, 10, 12, and 14, and v= (1 to 7). J. Chem. Thermodynamics 1999, 31, 151-176

[52] Hwu WH, Cheng JS, Cheng KW, Chen YP. Vapor-liquid equilibrium of carbon dioxide with ethyl caproate, ethyl caprylate and ethyl caprate at elevated pressures. Journal of Supercritical Fluids, 2004;28:1-9.

[53] Wang X, Wang X, Lang H. Measurement and correlation of density and viscosity of n-hexadecane with three fatty acid ethyl esters. J. Chem. Thermodynamics 2016;97:127–134.

[54] Xia J, Di G, Sun Y, Wang X, Yang X, He S. Volumetric properties of binary mixtures of methanol with ethyl caprylate, ethyl caprate, and ethyl laurate from 283.15 to 318.15 K. Energy Procedia 152 2018; 869–874

[55] Li D, Wang J, Gao Y, Zhan X, Li M, Wang Y. Density, Viscosity, and Refractive Index of Binary Mixtures of FattyAcid Ethyl Esters with Ethylcyclohexane. J. Chem. Eng. Data 2019;64:5324−5331.

[56] Ortega J. Measurements of excess enthalpies of {a methyl n-alkanoate (from n-hexanoate to n-pentadecanoate) +n-pentadecane} at 298.15 K. J. Chem. Thermodynamics 1990;22:1165-l 170.

[57] Liau WR, Tang M. Chen YP. Densities and viscosities of butyl acrylate plus 1-butanol and ethyl laurate plus 1-butanol at 293.15, 303.15, and 313.15 K. J. Chem. Eng. Data 1998;43:826–829.

[58] Smith RLJr, Yamaguchi T., Sato T., Suzuki H., Arai K. Volumetric behavior of ethyl acetate, ethyl octanoate, ethyl laurate, ethyl linoleate, and fish oil ethyl esters in the presence of supercritical CO2. Journal of Supercritical Fluids 1998;13: 29–36.

[59] Cheng KW, Tang M, Chen YP. Vapor–liquid equilibria of carbon dioxide with diethyl oxalate,ethyl laurate, and dibutyl phthalate binary mixtures at elevated pressures. Fluid Phase Equilibria 2001;181:1–16.

[60] Yang F, Wang X, Tan H, He S, Liu Z. Experimental investigations on the thermophysical properties of methyl myristate in alcoholic solutions. Fuel 2018;215:187–195.

[61] Komoda M, Harada I. Interaction of Tocored with Unsaturated Fatty Esters. J. Am. Oil Chem. Soc. 1970;47:249–253.

[62] Ott LS, Huber ML, Bruno TJ. Density and Speed of Sound Measurements on Five Fatty Acid Methyl Esters at 83 kPa and Temperatures from 278.15 to 338.15; K. J. Chem. Eng. Data 2008;53:2412–2416.

554 [63] Yuan Z, Zhao G, Yin J, Ma S. Study on thermophysical propertiesof methyl palmitate
555 and ethyl palmitate at high temperature. Chinese Internal Combustion Engine
556 Engineering 2019;40:67-73.
557 [64] Boelhouwer JWM, Nederbragt GW Verberg G. Viscosity data of organic liquids. Appl.
558 sci. Res. 1951;2, 249-268.
559 [65] Watanabe Y. Isomerization of Unsaturated Fatty Acids and their Esters with Acetic or
560 Inorganic Acid. Bulletin of the Chemical Society of Japan 1960;33:1319-1323.
561 [66] Knegtel JT, Boelhouwer C, Tels M, Waterman HI. Shifting of the double bond in
562 methyl oleate during hydrogenation. J Am Oil Chem Soc 1957;34:336–337.
563 [67] Candy L, Vaca-Garcia C, Borredon E. Synthesis and Characterization of Oleic Succinic
564 Anhydrides: Structure–Property Relations. JAOCS 2005;82:271-277.
565 [68] Elbro HS, Fredenslund A, Rasmussen P. Group contribution method for the prediction
566 of liquid densities as a function of temperature for solvents, oligomers, and polymers.
567 Ind Eng Chem Res 1991;30:2576–82.
568 [69] Ihmels EC, Gmehling J. Extension and revision of the group contribution method
569 GCVOL for the prediction of pure compound liquid densities. Ind Eng Chem Res
570 2003;42:408–12.
571 [70] Habrioux M, Freitas SVD, Coutinho JAP, Daridon JL. High Pressure Density and
572 Speed of Sound in Two Biodiesel Fuels. J. Chem. Eng. Data 2013;58:3392−3398.
573 [71] Kiełczynski P., Ptasznik S., Szalewski M., Balcerzak A., Wieja K., Rostocki A.J.
574 Thermophysical properties of rapeseed oil methyl esters (RME) at high pressures and
575 various temperatures evaluated by ultrasonic methods. Biomass and Bioenergy
576 2017;107:113-121.

577 [72] Ivaniš GR, Radovic IR, Veljkovic VB, Kijevcanin MLj. Biodiesel density and derived
578 thermodynamic properties at high pressures and moderate temperatures. Fuel
579 2016;165:244–251.
580 [73] Aitbelale R, Chhiti Y, M'hamdi Alaoui FE, Eddine AS, Munoz Rujas N, Aguilar F.
581 High-Pressure Soybean Oil Biodiesel Density: Experimental Measurements, Correlation
582 by Tait Equation, and Perturbed Chain SAFT (PC-SAFT) Modeling. J. Chem. Eng.
583 Data 2019;64:3994−4004.
584 [74] Bessières D, Bazile JP, Nguyen Thi Tanh X, García-Cuadrac F, Acien FG.
585 Thermophysical behavior of three algal biodiesels over wide ranges of pressure and
586 temperature. Fuel 233 2018; 497–503
587 [75] NguyenThi TX, Bazile JP, Bessières D. Density Measurements ofWaste Cooking Oil
588 Biodiesel and Diesel Blends Over Extended Pressure and Temperature Ranges.
589 Energies 2018;11:1212
590 [76] Aitbelale R, Abala I, M'hamdi Alaoui FE, Eddine AS, Munoz Rujas N, Aguilar F.
591 Characterization and determination of thermodynamic properties of waste cooking oil
592 biodiesel: Experimental, correlation and modeling density over a wide temperature
593 range up to 393.15 and pressure up to 140 MPa. Fluid Phase Equilibria 2019;49787-
594 49796.
595 [77] Tammann G. Ueber die Abhägigkeit der Volumina von Löungen vom Druck. Z. Phys.
596 Chem. 1895 ;17U : 620−636.
597 [78] Knothe G. Fuel Properties of Highly Polyunsaturated Fatty Acid Methyl Esters.
598 Prediction of Fuel Properties of Algal Biodiesel. Energy Fuels 2012 ;26 :5265−5273.
599

Table 1.
High pressure density data of liquid Fatty Acids Methyl Ester (FAME) and Fatty Acids Ethyl Ester (FAEE).

	First author Ref	Year	Temperature range/K	Pressure range/MPa	Number of data	Technique
FAME						
Caprate	Ndiaye [20]	2012	293-393	0.1-100	120	U- Tube
C10:0	Ndiaye [20]	2012	293-323	0.1-210	241	Speed of sound
	Zarska [21]	2014	293-318	0.1-100	66	Speed of sound
	Su [22]	2018	293-323	0.1-20	30	Flowmeter
Laurate	Tat [23]	2003	293-373	0.1-35	35	PVT cell
C12:0	Pratas [13]	2011	283-333	0.1-45	84	U- Tube
	Zarska [21]	2014	293-318	0.1-100	65	Speed of sound
	Wang [24]	2016	283-363	0.1-60	117	U- Tube
	Aissa [25]	2017	293-413	0.1-60	210	U- Tube
	Habrioux [26]	2018	293-353	0.1-200	53	Speed of sound
	He [27]	2018	303-353	0.1-15	36	Flowmeter
Myristate	Pratas [13]	2011	293-333	0.1-45	70	U- Tube
C14:0	Ndiaye [28]	2013	303-393	0.1-80	90	U- Tube
	Zarska[21]	2014	293-318	0.1-90	40	Speed of sound
Palmitate	Tat [23]	2003	293-373	0.1-35	35	U- Tube
C16:0	Ndiaye [28]	2013	313-383	0.1-70	90	U- Tube
	Rasulov [29]	2018	365-442	1-20	42	piezometer
Stearate C18:0	Tat [23]	2003	293-373	0.1-35	35	PVT cell
Oleate	Pratas [13]	2011	293-333	0.1-45	70	U- Tube
C18:1	Outcalt [30]	2011	270-470	.08-50	132	U- Tube
	Ndiaye[31]	2013	293-393	0.1-100	121	U- Tube
	Ndiaye[31]	2013	293-393	0.1-210	241	Speed of sound
Linoleate	Outcalt[30]	2011	270-370	.08-50	132	U- Tube
C18:2	Schedemann[32]	2013	278-367	.4-60	130	U- Tube
	Schedemann[32]	2013	278-337	.4-130	189	U- Tube
	Ndiaye[31]	2013	293-393	0.1-100	121	U- Tube
	Ndiaye[31]	2013	293-393	0.1-210	242	Speed of sound
FAEE						
Caprate	Ndiaye[20]	2012	293-393	0.1-100	121	U- Tube
C10:0	Ndiaye[20]	2012	293-323	0.1-210	242	Speed of sound
	Dzida [33]	2013	293-318	0.1-100	66	Speed of sound
Laurate	Dzida [34]	2013	293-318	0.1-100	66	Speed of sound
C12:0	Wang [24]	2016	283-363	0.1-60	117	U- Tube
	Aissa [25]	2017	293-413	0.1-60	210	U- Tube
	Habrioux [26]	2018	293-fr353	0.1-200	60	Speed of sound

	He [27]	2018	303-353	0.1-15	36	Flowmeter
Myristate	Ndiaye [28]	2013	303-393	0.1-100	117	U- Tube
C14:0	Dzida [34]	2013	293-318	0.1-100	56	Speed of sound
	Aissa [25]	2017	293-413	0.1-60	208	U- Tube
Oleate C18:1	Aissa [25]	2017	293-413	0.1-60	208	U- Tube

605
606
607

608 **Table 2**.

609 Atmospheric pressure density data of liquid Fatty Acids Methyl Ester (FAME) and Fatty

610 Acids Ethyl Ester (FAEE).

611

	First author	Year	T/K	Nb	First author	Year	T/K	Nb
	FAME				FAEE			
Caprate C10:0	Bonhorst [35]	1948	293-372	4	Gros [36]	1952	348	1
	Gros [36]	1952	348	1	Shigley [47]	1955	308-368	5
	Gouw [37]	1964	293-313	2	Smith[48]	1959	293	1
	Ortega [38]	1990	298	1	Liew[49]	1992	288-353	10
	Liew [39]	1992	283-353	15	Francesconi [50]	1998	293	1
	Pratas[40]	2010	278-363	18	Ortega[51]	1999	298	1
	Daridon [41]	2013	283-343	7	Hwu [52]	2004	293	1
	Wang [42]	2016	298-323	6	Pratas [40]	2010	283-353	15
	Sun [43]	2018	283-318	8	Daridon[41]	2013	283-373	10
	Du [44]	2019	298-333	8	Wang[53]	2016	298-323	6
	Li[45]	2019	298-323	6	Xia [54]	2018	283-318	8
	Zhao [46]	2019	293-453	17	Li [55]	2019	293-323	7
					Zhao[46]	2019	293-453	17
Laurate C12:0	Bonhorst [35]	1948	293-372	4	Gros[36]	1952	348	1
	Gros[36]	1952	348	1	Shigley[47]	1955	308-368	5
	Gouw [37]	1964	293-313	2	Liew[49]	1992	288-353	11
	Ortega[56]	1990	298	1	Liau [57]	1998	293	1
	Liew [39]	1992	283-353	15	Smith[58]	1998	313	1
	Pratas[40]	2010	283-353	15	Ortega[51]	1999	298	1
	Wang [42]	2016	298-323	6	Cheng[59]	2001	293	15
	Sun [43]	2018	283-318	8	Pratas[40]	2010	283-353	15
	Li[45]	2019	293-323	7	Wang[53]	2016	298-323	6
	Zhao [46]	2019	293-433	15	Xia [54]	2018	283-318	8
					Li [55]	2019	293-323	7
					Zhao[46]	2019	303-443	15
Myristate C14:0	Bonhorst [35]	1948	293-372	4	Gros[36]	1952	348	1
	Gros[36]	1952	348	1	Shigley[47]	1955	308-368	5
	Gouw [37]	1964	293-313	2	Liew[49]	1992	288-353	11
	Ortega[56]	1990	298	1	Ortega[51]	1999	298	1
	Liew[49]	1992	303-348	10	Pratas[40]	2010	283-353	15
	Pratas[40]	2010	298-353	12	Daridon[41]	2013	293-373	9
	Daridon[41]	2013	303-373	8	Li [55]	2019	293-323	7
	Wang [42]	2016	298-323	6	Zhao[46]	2019	293-443	16
	Sun [43]	2018	298-318	5				
	yang [60]	2018	303-333	7				
	Li[45]	2019	293-323	7				
	Zhao [46]	2019	293-413	13				
Palmitate	Bonhorst	1948	310-372	3	Boelhouwer	1951	298-573	6

	[35]				[64]			
C16:0	Gros[36]	1952	348	1	Gros[36]	1952	348	1
	Gouw [37]	1964	313	1	Shigley[47]	1955	308-368	5
	Komoda [61]	1970	323	1	Ortega[51]	1999	298	1
	Ott[62]	2008	308-338	7	Pratas[40]	2010	303-353	11
	Pratas[40]	2010	308-363	12	Yuan[63]	2019	333-547	12
	Daridon[41]	2013	313-373	7				
	Yuan[63]	2019	333-547	12				
Palmitoleate C16:1	Watanabe [65]	1960	298	1				
	Pratas[19]	2011	278-363	18				
Stearate	Bonhorst [35]	1948	310-372	3	Boelhouwer [64]	1951	323-513	5
	Boelhouwer [64]	1951	323-513	5	Gros[36]	1952	348	1
C18:0	Gros[36]	1952	348	1	Shigley[47]	1955	308-368	5
	Gouw [37]	1964	313	1	Pratas[40]	2010	313-363	11
	Liew [49]	1992	313-353	9				
	Ott [62]	2008	318-338	5				
	Pratas[40]	2010	313-363	11				
Oleate	Knegtel [66]	1957	293	1	Candy [67]	2005	293.15	1
	Watanabe [65]	1960	298	1	Pratas[40]	2010	278-363	18
C18:1	Gouw [37]	1964	293-313	2				
	Komoda [61]	1970	298	1				
	Candy [67]	2005	293	1				
	Ott [62]	2008	278-338	7				
	Pratas[40]	2010	278-363	18				
	Daridon [41]	2013	283-373	10				
Linoleate	Gouw [37]	1964	293-313	2	Smith [58]	1998	313	1
	Komoda [61]	1970	298	1	Pratas[19]	2010	278-363	18
C18:2	Ott [62]	2008	278-338	7				
	Pratas [40]	2010	278-363	18				
	Daridon [41]	2013	283-373	10				
Linolenate C18:3	Gouw [37]	1964	293-313	2	Pratas[19]	2010	278-373	20
	Ott [62]	2008	278-338	7				
	Pratas[19]	2010	278-363	18				
Arachidate C20:0	Gouw [37]	1964	313	1	Pratas[19]	2011	318-373	12
	Pratas[19]	2011	323-373	11				
Gadoleate C20:1	Pratas[19]	2011	278-373	20				
Behenate C22:0	Pratas[19]	2011	333-373	9				
Erucate C22:1	Gouw [37]	1964	293-313	2				
	Pratas[19]	2011	278-363	18				
Lignocerate C24:0	Pratas[19]	2011	338-373	8				

612 **Table 3**.

Group contribution values for parameters of eqs. 2-3, 6-8 where the units are K for the temperature T, MPa for pressure p and $cm^3.mol^{-1}$ for volume increments $v_j(T,p)$.

	a_0	$a_1 \times 10^3$	$a_2 \times 10^6$	$b_0 \times 10^3$	$b_1 \times 10^6$	$b_2 \times 10^9$	$c_0 \times 10^3$	$c_1 \times 10^6$
CH3	16.43000	55.62000	0	141.0915	-937.170	1786.650	-18.02781	-416.5600
CH2	12.04000	14.10000	0	1.828686	-7.32110	8.242550	673.4669	-5335.580
CH=CH	43.17037	-99.28637	155.2190	4.549329	-31.8870	59.77000	-2910.446	5352.666
CH_3COO	45.86310	-3.709090	83.30000	44.79574	-151.000	165.7020	198.9688	-910.8600
C_2H_5COO	68.40212	-40.28484	159.8240	80.85027	-350.450	428.5890	249.4559	-1084.450

620 **Table 4**

621 Parameters of Murnaghan equation [17] of pure Fatty Acid Methyl Esters and Fatty Acid
622 Ethyl Esters used in eq. 15 where the units are K for the temperature T, MPa for pressure p
623 and $cm^3.mol^{-1}$ for volume $v(T,p)$.

624

	a_0	$a_1 \times 10^3$	$a_2 \times 10^6$	$b_0 \times 10^3$	$b_1 \times 10^6$	$b_2 \times 10^9$	$c_0 \times 10^3$	$c_1 \times 10^6$
FAME								
C10:0	167.8959	106.7739	166.9610	20.75502	-131.7700	297.3830	-97.64292	-15.01000
C12:0	198.5288	103.4472	206.0360	13.35048	-87.15400	232.0300	-101.6336	15.80980
C14:0	221.4977	143.5773	184.2740	17.60627	-119.0600	297.7900	-105.9907	57.67670
C16:0	253.8070	124.4893	255.0380	24.99391	-166.2200	360.1700	-129.2231	117.9640
C16:1	246.7464	152.5615	202.8800	8.527390	-52.22200	142.8670	-127.4771	28.27370
C18:0	258.6963	273.2155	69.19890	8.132622	-45.43100	123.5910	-135.3409	73.08580
C18:1	280.9855	117.4477	276.2360	14.03595	-78.61400	184.0230	-88.57095	-41.54900
C18:2	274.0727	123.8887	255.2240	11.17410	-54.61100	139.6520	-66.27109	-98.65500
C18:3	302.2871	-95.36963	585.8010	10.26528	-70.31300	170.1990	-172.6542	85.72460
C20:0	270.5583	375.1460	-40.78100	7.517432	-40.84400	110.5550	-145.1129	92.86160
C20:1	313.5710	95.65575	346.5100	7.681347	-45.04300	119.4270	-150.9487	83.34940
C22:0	277.7420	485.0573	-136.9800	6.946821	-36.68300	99.12680	-154.1908	110.1740
C22:1	323.6248	222.8248	186.2350	7.186587	-41.16200	108.5260	-160.8404	104.4310
C24:0	313.6635	464.3115	-88.70100	6.425814	-32.95100	89.11600	-162.6810	125.4520
FAEE								
C10:0	180.6837	124.4817	170.1120	4.639978	-17.95200	104.5670	-54.81752	-141.3800
C12:0	212.4059	115.9065	214.9730	4.976450	-32.75200	145.0720	-92.82938	-15.31200
C14:0	242.3230	115.3258	252.1790	12.42137	-66.50300	172.5440	-70.87564	-86.47500
C16:0	264.2868	162.0671	218.6960	4.164460	-15.18400	75.66210	-93.48324	-45.96500
C16:1	272.4825	85.24879	315.0430	3.146145	-10.00500	66.60260	-83.06140	-103.8100
C18:0	282.5838	228.2740	159.7660	4.292851	-16.17200	71.93060	-104.8864	-19.66100
C18:1	292.5633	139.9768	272.0640	7.814890	-52.22200	162.9790	-111.4736	27.66500
C18:2	285.3669	148.0623	242.2020	2.697067	-8.920400	60.16880	-87.92858	-122.5800
C18:3	277.2908	162.6322	211.0990	1.626377	-2.126800	47.58790	-70.13632	-203.6600
C20:0	299.6463	302.3346	86.89330	4.312686	-16.39100	67.72530	-115.2614	3.007290
C20:1	320.6425	141.6488	315.0430	3.820384	-15.23000	66.75190	-111.2576	-33.13800
C22:0	325.6321	297.3352	159.8240	4.316140	-16.60800	64.30960	-125.5823	24.99000
C22:1	344.7225	169.8488	315.0430	3.930681	-16.05400	64.50450	-122.7918	-6.357800
C24:0	349.7121	325.5352	159.8240	4.240813	-16.22100	60.35050	-134.8461	43.56520

625

Table 5.

Statistical characteristics (Average Deviations, Average Absolute Deviations, Maximum Deviation) for the predictions of the effect of pressure ρ/ρ_{atm} on FAME and FAEE pure components from eqs. 1-3 using parameters given in Table 4.

	First author	AD %	AAD %	MD %	First author	AD %	AAD %	MD %
FAME					FAEE			
Caprate	Ndiaye[1] [20]	0.02	0.04	0.17	Ndiaye[1] [20]	0.01	0.05	0.14
C10:0	Ndiaye[2] [20]	0.004	0.03	0.10	Ndiaye[2] [20]	0.004	0.02	0.07
	Zarska [21]	-0.03	0.03	0.06	Dzida [33]	-0.02	0.02	0.07
	Su [22]	0.10	0.12	0.56				
Laurate	Tat [23]	-0.01	0.02	0.06	Dzida [34]	-0.03	0.03	0.08
C12:0	Pratas [13]	0.001	0.01	0.03	Wang [24]	0.01	0.03	0.10
	Zarska [21]	-0.01	0.05	0.25	Aissa [25]	0.004	0.03	0.21
	Wang [24]	-0.02	0.02	0.21	Habrioux [26]	-0.03	0.05	0.23
	Aissa [25]	0.00	0.02	0.16				
	Habrioux [26]	-0.04	0.06	0.30				
	He [27]	0.02	0.02	0.08				
Myristate	Pratas [13]	0.02	0.02	0.05	Ndiaye [28]	0.00	0.03	0.12
C14:0	Ndiaye [28]	-0.03	0.09	0.40	Dzida [34]	-0.02	0.02	0.06
	Zarska [21]	-0.03	0.03	0.11	Aissa [25]	0.01	0.02	0.08
Palmitate	Tat [23]	-0.08	0.08	0.16				
C16:0	Ndiaye [28]	-0.07	0.07	0.33				
	Rasulov[29]	-0.14	0.15	0.60				
Stearate C18:0	Tat [23]	-0.24	0.24	0.71				
Oleate	Pratas [13]	-0.01	0.01	0.03				
C18:1	Outcalt [30]	-0.01	0.02	0.10				
	Ndiaye[1] [31]	0.01	0.03	0.07				
	Ndiaye[2] [31]	-0.01	0.02	0.05				
Linoleate	Outcalt [30]	-0.01	0.02	0.12				
C18:2	Schedemann [32]	-0.01	0.02	0.05				
	Schedemann [32]	-0.02	0.02	0.08				
	Ndiaye[1] [31]	0.02	0.03	0.14				
	Ndiaye[2] [31]	0.01	0.02	0.08				

[1] obtained from U-tube vibrating densimeter

[2] obtained from speed of sound integration

636 **Table 6**.

637 Fatty Acid Alkyl Ester profiles in mol% of different oil and fat biodiesels used for testing the

638 predictive capacity of the proposed method.

639

Biodiesel* / Author		C1 0:0	C1 2:0	C1 4:0	C1 6:0	C1 6:1	C1 8:0	C1 8:1	C1 8:2	C1 8:3	C2 0:0	C2 0:1	C2 2:0	C2 2:1	C2 4:0
Methyl															
C	Tat [23]	0.0	0.0	0.0	4.3	0.2	1.9	65.0	19.1	9.5	0.0	0.0	0.0	0.0	0.0
Ct	Prieto [14]	0.0	0.0	1.1	28.4	0.0	2.7	17.3	50.5	0.0	0.0	0.0	0.0	0.0	0.0
Ls1	Tat [23]	0.0	0.0	0.0	22.4	0.0	27.4	15.0	7.5	27.7	0.0	0.0	0.0	0.0	0.0
Ls2	Tat [23]	0.0	0.0	0.0	40.9	0.0	42.3	4.6	2.3	9.9	0.0	0.0	0.0	0.0	0.0
P	Pratas [13]	0.0	0.3	0.7	44.6	0.1	3.8	40.3	9.5	0.1	0.3	0.1	0.1	0.0	0.1
R	Pratas [13]	0.0	0.1	0.1	5.7	0.2	1.6	61.8	21.1	7.0	0.5	1.2	0.3	0.2	0.2
R	Habrioux [70]	0.0	0.1	0.1	5.7	0.2	1.6	61.8	21.1	7.0	0.5	1.2	0.3	0.2	0.2
R	Kiełczynski [71]	0.0	0.0	0.1	5.0	0.4	1.8	60.6	20.0	9.2	0.5	1.5	0.2	0.4	0.3
S	Tat [23]	0.0	0.0	0.1	11.9	0.1	3.9	23.1	53.1	7.8	0.0	0.0	0.0	0.0	0.0
S	Pratas [13]	0.0	0.0	0.1	11.6	0.1	3.9	22.7	53.2	7.0	0.3	0.2	0.7	0.2	0.0
S	Habrioux [70]	0.0	0.0	0.1	11.6	0.1	3.9	22.7	53.2	7.0	0.3	0.2	0.7	0.2	0.0
S	Ivaniš [72]	0.0	0.0	0.1	8.7	0.0	3.2	28.9	58.9	0.0	0.0	0.0	0.0	0.2	0.0
S	Aitbelale [73]	0.0	0.0	0.0	12.1	0.0	4.0	23.6	53.2	7.1	0.0	0.0	0.0	0.0	0.0
S^H	Tat [23]	0.0	0.0	0.0	12.3	0.0	87.7	0.0	0.0	0.0	0.0	0.0	0.0	0.0	0.0
S^O	Tat [23]	0.0	0.0	0.0	16.4	0.0	5.2	56.1	22.3	0.0	0.0	0.0	0.0	0.0	0.0
Asp	Bessières [74]	0.0	0.0	5.3	45.7	9.2	2.5	1.7	21.8	13.8	0.0	0.0	0.0	0.0	0.0
L	Tat [23]	0.0	0.1	1.8	27.2	3.4	12.2	45.2	10.0	0.1	0.0	0.0	0.0	0.0	0.0
L	Ivaniš [72]	0.0	0.0	0.0	30.5	0.0	16.4	42.3	10.4	0.2	0.0	0.0	0.0	0.2	0.0
T	Tat[23]	0.0	0.1	4.1	28.4	3.8	21.7	39.1	2.2	0.6	0.0	0.0	0.0	0.0	0.0
W	NguyenThi [75]	0.0	0.0	3.8	26.9	7.7	12.8	36.7	9.6	0.0	0.5	2.0	0.0	0.0	0.0
W	Aitbelale [76]	0.0	0.0	67.4	0.0	0.0	0.0	24.5	7.4	0.7	0.0	0.0	0.0	0.0	0.0
BP	Schedemann [32]	0.0	0.0	0.6	8.6	0.2	2.2	58.1	20.5	8.1	0.4	1.0	0.1	0.1	0.1
RP	Pratas [13]	0.0	0.3	0.6	24.7	0.2	2.9	51.8	15.2	3.0	0.4	0.6	0.2	0.1	0.0
SP	Pratas [13]	0.0	0.2	0.0	27.3	0.1	3.9	32.3	31.3	3.5	0.3	0.2	0.3	0.1	0.5
SR	Pratas [13]	0.0	0.0	0.1	9.7	0.2	2.7	41.4	37.4	7.0	0.4	0.6	0.4	0.1	0.0
SRP	Pratas [13]	0.0	0.2	0.5	20.4	0.2	3.2	41.6	27.6	4.6	0.4	0.5	0.3	0.1	0.4
Ethyl															
S	Tat [23]	0.0	0.0	0.0	15.1	0.0	8.8	52.0	24.1	0.0	0.0	0.0	0.0	0.0	0.0
S	Ivaniš [72]	0.0	0.0	0.1	8.7	0.0	3.2	29.0	59.0	0.0	0.0	0.0	0.0	0.0	0.0
S^H	Tat [23]	0.0	0.0	0.0	12.9	0.0	87.1	0.0	0.0	0.0	0.0	0.0	0.0	0.0	0.0
S^O	Tat [23]	0.0	0.0	0.1	11.9	0.1	3.9	23.2	53.0	7.8	0.0	0.0	0.0	0.0	0.0

640 * C: canola, Ct: cottonseed, Ls: linseed, P: palm, R: rapeseed, S: soybean, Asp: alga spirulina

641 platensis, L: lard, T: tallow, W: waste cooking oils, PB: purified biodiesel, PR: palm + rapeseed

642 blend, SR: soybean + rapeseed blend, SP: soybean + palm blend, SRP: soybean + rapeseed + palm

643 blend, ^{H} Hydrogenated, ^{O} : Oxidized.

644

Table 7.

Statistical Characteristics (Average Deviations, Average Absolute Deviations, Maximum Deviation) for the prediction of the effect of pressure on biodiesel densities from eq. 15 using parameters given in Table 4.

Biodiesel* / First author		Year	AD	AAD	MD	T range /K	P range /MPa	Ur(ρ) %	Number of data
Methyl									
C	Tat [23]	2003	0.01	0.03	0.09	293-373	0.1-35	0.2	30
Ct	Prieto [14]	2015	0.01	0.02	0.11	288-358	0.1-30	0.17	120
Ls1	Tat [23]	2003	-0.01	0.03	0.12	293-373	34.5	0.2	30
Ls2	Tat [23]	2003	-0.05	0.06	0.26	293-373	34.5	0.2	30
P	Pratas [13]	2011	0.007	0.01	0.06	283-333	0.1-45	0.02	84
R	Pratas [13]	2011	0.005	0.01	0.05	283-333	0.1-45	0.02	84
R	Habrioux [70]	2013	0.14	0.14	0.28	293-393	0.1-200	0.3	231
R	Kiełczynski [71]	2017	4.42	4.42	8.05	278-293	0.1-250	0.2	104
S	Tat [23]	2003	0.01	0.03	0.09	293-373	0.1-35	0.2	30
S	Pratas [13]	2011	0.02	0.02	0.07	283-333	0.1-45	0.02	84
S	Habrioux [70]	2013	0.03	0.05	0.13	293-393	0.1-200	0.3	231
S	Ivaniš [72]	2016	0.03	0.03	0.12	288-413	0.1-60	0.1	222
S	Aitbelale [73]	2019	0.04	0.05	0.14	298-393	0.1-140	0.1	136
S^H	Tat [23]	2003	-0.13	0.13	0.38	293-373	0.1-35	0.2	30
S^O	Tat [23]	2003	0.03	0.04	0.10	293-373	0.1-35	0.2	30
Asp	Bessières [74]	2018	0.01	0.02	0.05	293-353	0.1-140	0.1	51
L	Tat [23]	2003	-0.01	0.04	0.12	293-373	0.1-35	0.2	30
L	Ivaniš [72]	2016	-0.04	0.04	0.18	298-413	0.1-60	0.1	194
T	Tat[23]	2003	-0.05	0.06	0.22	293-373	0.1-35	0.2	30
W	NguyenThi [75]	2018	0.46	0.46	0.94	293-353	0.1-140	0.1	60
W	Aitbelale [76]	2019	0.20	0.20	0.39	298-393	0.1-140	0.1	136
BP	Schedemann [32]	2013	-0.02	0.03	0.06	288-397	0.1-130	0.1	324
RP	Pratas [13]	2011	0.004	0.006	0.02	283-333	0.1-45	0.02	84
SP	Pratas [13]	2011	0.003	0.01	0.04	283-333	0.1-45	0.02	84
SR	Pratas [13]	2011	0.02	0.02	0.06	283-333	0.1-45	0.02	84
SRP	Pratas [13]	2011	0.001	0.004	0.01	283-333	0.1-45	0.02	84
Ethyl									
S	Tat [23]	2003	-0.08	0.08	0.25	293-373	0.1-35	0.2	30
S	Ivaniš [72]	2016	0.008	0.02	0.14	288-373	0.1-60	0.1	196
S^H	Tat [23]	2003	-0.1	0.1	0.4	293-373	0.1-35	0.2	30
S^O	Tat [23]	2003	-0.004	0.03	0.09	293-373	0.1-35	0.2	30

* C: canola, Ct: cottonseed, Ls: linseed, P: palm, R: rapeseed, S: soybean, Asp: alga spirulina platensis, L: lard, T: tallow, W: waste cooking oils, PB: purified biodiesel, PR: palm + rapeseed blend, SR: soybean + rapeseed blend, SP: soybean + palm blend, SRP: soybean + rapeseed + palm blend, ^{H} Hydrogenated, ^{O} : Oxidized.

Fig. 1. Relative density deviations between the calculated density values with the proposed method (eq. 15) and the experimental literature values for soy bean oil methyl biodiesel at T = 313 K: ✚, Tat and Van Gerpen [23]; ✖, Pratas et al. [13]; ■, Habrioux et al. [70]; ●, Ivaniš et al. [72]; Δ, Aitbelale et al. [73].

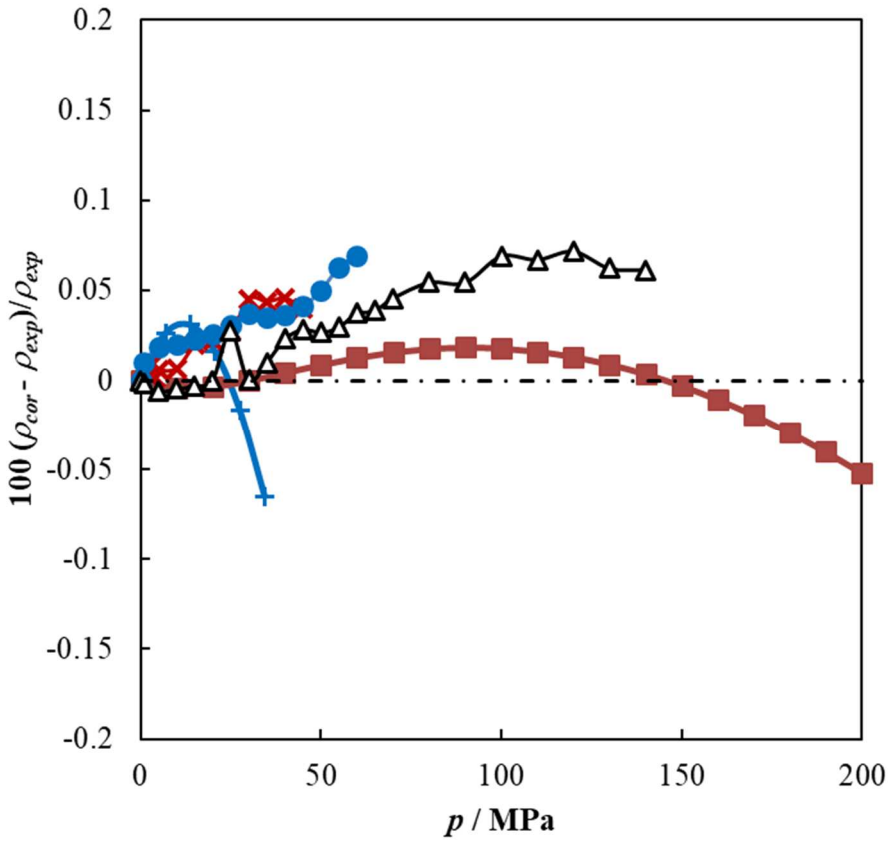

Fig. 2. Relative density deviations between the calculated values with the proposed method (eq. 15) and the experimental literature values of vaniš et al. [72] for soy bean oil ethyl biodiesel at different temperatures: ■, 293 K ; Δ, 303 K; ●, 313 K; ×, 323 K; □, 333 K; +, 353 K; ◆, 363 K; ○, 373 K

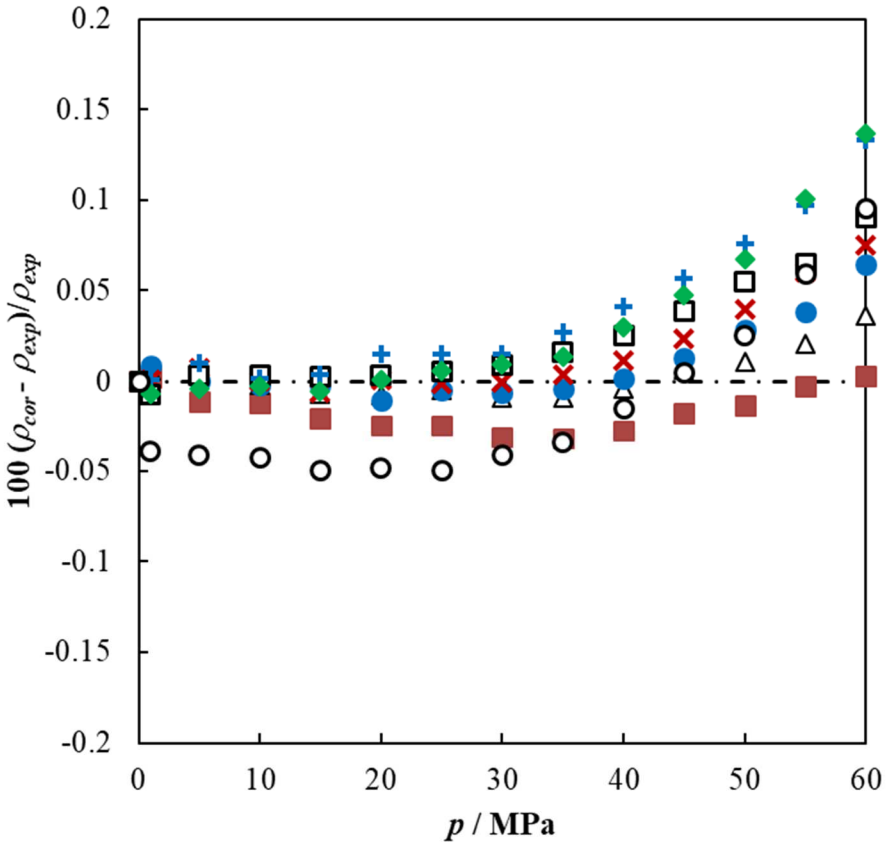

711 **Fig. 3.** Comparison of the density deviations obtained from eqs. 15 and 16 for two methyl
712 biodiesels at T= 298 K: Δ , soy bean oil biodiesel [73] with eq. 15; ▲ soy bean oil biodiesel
713 [73] with eq. 16: ○ , purified biodiesel [32] with eq. 15; ●, purified biodiesel [32] with eq.
714 16.

715
716
717

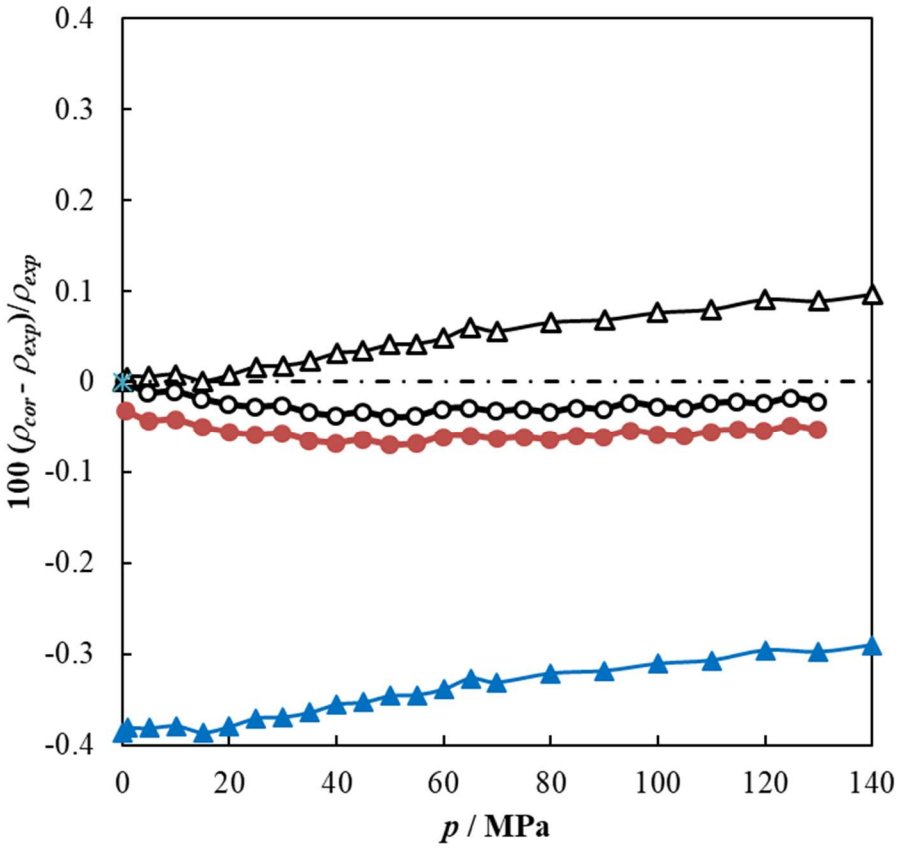

718
719
720
721
722

Fig. 4. Relative compressibility deviations between the calculated values with the proposed method (eqs. 17, 18) and the literature values obtained from fitting a Tait like equation of state for soy bean oil methyl biodiesel at T = 313 K: ✖, Pratas et al. [13]; ■, Habrioux et al. [70]; ●, Ivaniš et al. [72]; Δ, Aitbelale et al. [73].